

Magnetic susceptibility and heat capacity investigations of the unconventional spin-chain compound $\text{Sr}_3\text{CuPtO}_6$

S. Majumdar, V. Hardy,* M. R. Lees, and D. McK. Paul

Department of Physics, University of Warwick, Coventry CV4 7AL, United Kingdom

H. Rousselière and D. Grebille

Laboratoire CRISMAT, UMR 6508, Boulevard du Maréchal Juin, 14050 Caen cedex, France

(Received 14 August 2003; revised manuscript received 1 October 2003; published 15 January 2004)

The Heisenberg spin-chain compound $\text{Sr}_3\text{CuPtO}_6$ is investigated by magnetic susceptibility and heat capacity measurements. $\text{Sr}_3\text{CuPtO}_6$ has an unconventional chain structure in the sense that (i) the spin-half copper atoms are arranged in a zigzag chain structure and (ii) neighboring Cu atoms along the chains are separated by spin-zero platinum atoms. We report that this compound shows broad features in the temperature dependence of both the magnetic contribution to the heat capacity and the magnetic susceptibility. Despite the unconventional nature of the spin-chain structure, this set of data exhibits good agreement with theoretical models for a classical $S = \frac{1}{2}$ Heisenberg spin-chain compound. The values of the intrachain coupling constant, obtained by different techniques, are found to be very close to each other. The low-temperature heat capacity data (below ~ 6 K) exhibit a deviation from the theoretically expected behavior, which could be related to a small energy gap in the spin excitation spectrum.

DOI: 10.1103/PhysRevB.69.024405

PACS number(s): 75.40.Cx, 75.50.Ee, 75.10.Pq

I. INTRODUCTION

A new class of one-dimensional (1D) magnetic compounds with the general formula A_3XYO_6 ($A = \text{Sr}, \text{Ca}$; $X, Y =$ transition metals) has attracted particular interest recently.¹ These materials crystallize in a K_4CdCl_6 -type rhombohedral structure, which consists of infinite chains built up of alternating face-sharing YO_6 octahedra and XO_6 trigonal prisms. These YO_6 - XO_6 chains are separated from each other by A^{2+} cations and constitute a hexagonal cross-sectional arrangement perpendicular to the chain direction. Depending upon the nature and the oxidation states of the cations at the X and the Y sites, these materials present a range of low-dimensional magnetic phenomena.² In this class of materials, $\text{Sr}_3\text{CuPtO}_6$ is reported to be a spin-half Heisenberg antiferromagnet (AFM) chain compound.²⁻⁴

From a crystallographic point of view, $\text{Sr}_3\text{CuPtO}_6$ does not constitute an ideal linear spin-chain structure.⁵ First, due to the presence of Cu^{2+} cations at the X site, the K_4CdCl_6 -type rhombohedral structure undergoes a monoclinic distortion. The Pt^{4+} ions stay at the center of the PtO_6 octahedra maintaining a linear structure, whereas the Cu^{2+} ions move from the center of the CuO_6 trigonal prisms to their faces. Successive Cu^{2+} ions on a chain are displaced away from the chain axis in opposite directions, resulting in a zigzag chain structure with a Cu-Cu bond angle of 160.94° (see Fig. 1). Second, along each chain, neighboring $S = \frac{1}{2}$ Cu^{2+} ions are separated by a Pt^{4+} ion. In the presence of a strong octahedral crystal field, the Pt^{4+} ions adopt a low-spin ground state with zero effective spin. This results in a $\frac{1}{2}$ -0- $\frac{1}{2}$ -0- $\frac{1}{2}$... type of spin-chain structure in which the $S = \frac{1}{2}$ interspin separations parallel and perpendicular to the chains are almost equal. Prompted by this fact, Claridge *et al.*³ analyzed the magnetic susceptibility data of $\text{Sr}_3\text{CuPtO}_6$ considering both intrachain (J) and interchain

(J') couplings among the Cu^{2+} ions. From their analysis, using a modified Bonner and Fisher model,⁶ they reported that $J = 24.7$ K and $J' = 7.3$ K. Since $J/J' \sim 3$, they concluded that the compound should not be considered as a 1D magnetic system. However, the broad maximum observed in the magnetic susceptibility data^{2,3} gives a strong indication that the compound does indeed have the characteristics of a low-dimensional magnetic system. As a result, the magnetic status of $\text{Sr}_3\text{CuPtO}_6$ remains unclear.

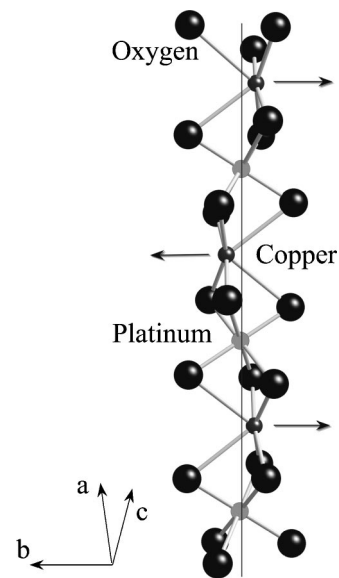


FIG. 1. A single CuO_6 - PtO_6 chain in the crystal structure of $\text{Sr}_3\text{CuPtO}_6$. The line through the platinum atoms indicates the direction of the chain axis. The arrows indicate the displacement of the copper atoms from the chain axis resulting in the formation of a zigzag chain structure. Each chain is separated from the others by the Sr^{2+} ions.

In this paper, we present the results of a thorough investigation of the magnetic susceptibility and heat capacity behavior of single-crystal samples of $\text{Sr}_3\text{CuPtO}_6$. While there have been studies of the magnetic susceptibility of this compound,^{2,3,7} the present paper reports on a combined investigation of the heat capacity and the magnetic susceptibility of this material. Despite the fact that heat capacity can provide important information about the magnetic character of spin-chain systems, very little heat capacity data have been published to date for the A_3XYO_6 class of compounds.^{8,9}

The theoretical model of Bonner and Fisher has been successfully used in the past to fit the experimental susceptibility data for $S = \frac{1}{2}$ spin-chain systems.¹⁰ This model is based on the extrapolation of numerical calculations for a finite number of spins (≤ 11) and is valid in a limited temperature range ($T \geq \frac{1}{2}J$, where J is the intrachain coupling constant in kelvin). Recently Klümper, Johnston, and co-workers^{11,12} have used the Bethe ansatz approach to formulate a model for the $S = \frac{1}{2}$ Heisenberg spin-chain system, which should be valid over the entire temperature range. This model is an extension of previous theoretical work.^{13,14} In the present paper, the majority of the fitting has been carried out using this new analytical model proposed by Johnston and co-workers (hereafter called the Johnston model).¹¹ The Bonner-Fisher model has also been used for comparison. Throughout the paper, we have adopted the convention where the spin Hamiltonian \mathcal{H} is defined as $\mathcal{H} = 2Jk_B \sum_i \mathbf{S}_i \cdot \mathbf{S}_{i+1}$, where \mathbf{S}_i is the i th spin on the chain and k_B is the Boltzmann constant.

II. EXPERIMENTAL DETAILS

The needle shaped crystals of $\text{Sr}_3\text{CuPtO}_6$ used in this investigation were prepared by a K_2CO_3 flux method as described in Ref. 3. The crystals were analyzed by x-ray diffraction using Mo K_α radiation on a Bruker-Nonius-Kappa charge-coupled device single-crystal x-ray diffractometer. The cell refinement showed that the crystals have a monoclinic structure (space group $C2/c$) with lattice parameters $a = 9.34(1)$ Å, $b = 9.64(1)$ Å, $c = 6.68(1)$ Å, and $\beta = 91.91(5)^\circ$, which are in good agreement with the literature.⁵ The rod axis of the crystals was found to be along the [201] direction, which coincides with the CuO_6 - PtO_6 chain direction. The magnetic susceptibility measurements were carried out using a Quantum Design superconducting quantum interference device magnetometer in the temperature (T) range 2–400 K with the applied magnetic field H parallel to the chain direction. The zero-field heat capacity C measurements were performed by a relaxation method using a Quantum Design physical properties measurement system. The C versus T data in the temperature range 1.9–300 K were recorded with a conventional ^4He insert, whereas the data collected below 1.9 K were recorded using a ^3He refrigerator option. Since the mass of each crystal is typically ~ 1 –2 mg, an assembly of six crystals, with their rod axis aligned, was used for both the magnetization (M) and the heat capacity measurements.

In order to obtain information about the short-range magnetic correlations from the heat capacity data, it is necessary

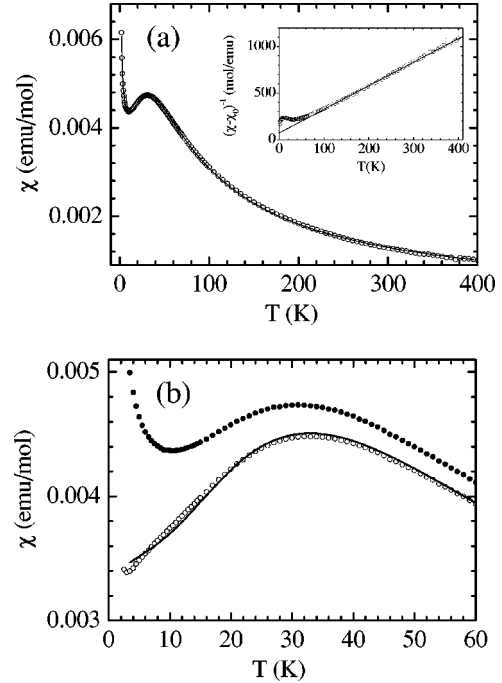


FIG. 2. The upper panel (a) shows the magnetic susceptibility vs temperature data in the temperature range 2–400 K with the applied field ($H = 10$ kOe) parallel to the [201] direction. The solid line through the data points is a global fit of the data using a Johnston term, a temperature-independent term, and a Curie term (as discussed in the text). The inset in the upper panel shows the inverse susceptibility vs temperature data with the temperature-independent term χ_0 removed. The solid line in the inset shows a linear fit of the data in the temperature range 250–400 K. The lower panel (b) shows the low-temperature (2–60 K) behavior of the susceptibility with $H = 10$ kOe, applied parallel to the [201] direction. The data points with filled circles show the total susceptibility data, whereas the data points with open circles indicate susceptibility after the Curie contribution (χ_{add}) and the temperature-independent positive term (χ_0) have been subtracted. The solid line through the open circles shows a Johnston model fit associated with the spin-chain contribution (χ_{chain}).

to estimate the lattice contribution to the heat capacity C_{lat} . It is therefore important to measure a nonmagnetic reference compound with the same crystal structure and containing elements with similar masses. For this purpose, a ceramic sample of the isostructural compound $\text{Sr}_3\text{ZnPtO}_6$ was prepared by the usual solid-state reaction technique.¹⁵ This compound was found to be essentially nonmagnetic. The small Curie constant $c_{cw} \sim 2.6 \times 10^{-3}$ emu/K mol, derived from the magnetic susceptibility versus temperature data for $\text{Sr}_3\text{ZnPtO}_6$, corresponds to only 0.1% of the Pt^{4+} ions on the prismatic sites being in the high-spin ($S = 2$) magnetic state.

III. RESULTS

A. Susceptibility

Figure 2 shows the magnetic susceptibility ($\chi = M/H$) versus temperature data of $\text{Sr}_3\text{CuPtO}_6$ in the temperature range 2–400 K with the applied magnetic field (10 kOe)

along the [201] direction. The low-temperature $\chi(T)$ data show a rise with decreasing temperature below 10 K, similar to that observed in a previous investigation³ on this compound. Such a feature has also been observed in a number of other spin-chain compounds^{16,17} and it is generally thought to arise from the presence of broken chains and/or paramagnetic impurities; both effects lead to a Curie-like term.¹⁸ At intermediate temperatures, the susceptibility versus temperature data show a broad peak around 32 K, which is typical of short-range magnetic order in a spin-chain system. The high-temperature data (250–400 K) show Curie-Weiss behavior along with a temperature-independent positive term χ_0 .

For a quantitative analysis of the susceptibility versus temperature data, we express χ as a sum of three terms as in Ref. 19 as

$$\chi = \chi_{add} + \chi_0 + \chi_{chain}. \quad (1)$$

The term $\chi_{add} = c_{add}/(T - \theta_{add})$ is a Curie-like term coming from broken chains or paramagnetic impurities in the system. The term χ_0 is a combination of the van Vleck paramagnetic term and the diamagnetic contributions from the atomic cores. χ_{chain} is the contribution coming from the 1D magnetic correlations among the spins. This can be approximated using the Johnston model [Eq. (50) of Ref. 11] for the $S = \frac{1}{2}$ uniform linear-chain system where we write $\chi_{chain}(T) = \chi\{J, g\}(T)$, J and g (Landé g factor) are the free parameters. With these considerations, we have fitted our $\chi(T)$ data to Eq. (1) in the temperature range 2–400 K (solid line in Fig. 2). The good quality of the fit over the full temperature range indicates that the Johnston model can be used to describe the susceptibility behavior of $\text{Sr}_3\text{CuPtO}_6$. The parameters obtained from the fitting are the following: $J = 25.7(1)$ K, $g = 2.050(3)$, $\chi_0 = 8.1(7) \times 10^{-5}$ emu/mol, $c_{add} = 0.0055(1)$ emu K/mol, and $\theta_{add} = -0.14(5)$ K. Similar fitting for $T > 13$ K ($\sim \frac{1}{2}J$), using the Bonner-Fisher model for χ_{spin} , produces a value of $J = 25.3(1)$ K, which compares well with the result obtained using the Johnston model. The value of J is also in good agreement with the value (26.1 K) estimated by Nguyen *et al.*⁴ using the Bonner-Fisher model.

The Curie constant associated with χ_{add} corresponds to a moment of $1.73\mu_B$ residing on $\sim 1.5\%$ of the Cu atoms present in the sample. The value of χ_{add} remains practically unchanged if one sets $\theta_{add} = 0$. This concentration of free Cu^{2+} ions is comparable with the values previously reported in some other Cu^{2+} based spin-chain compounds.^{16,17}

At high temperatures (250–400 K), the $1/[\chi(T) - \chi_0]$ versus T plot (see inset of the upper panel) is found to be linear with respect to T , when using the value of χ_0 obtained from the global fitting (2–400 K) of our data to Eq. (1). This is expected, because at high temperatures, χ_{add} becomes negligible and χ_{spin} reduces to a Curie-Weiss term. Additional confidence in the reliability of this χ_0 value comes from fitting the high-temperature $\chi(T) - \chi_0$ data to a simple Curie-Weiss expression, where one finds an effective moment $p_{eff} = 1.77(2)\mu_B/\text{Cu}^{2+}$, which is close to the theoretical value ($1.73\mu_B$), and a paramagnetic Curie tempera-

ture $\theta_p = -26(\pm 2)$ K that compares well with the J value as expected for an $S = \frac{1}{2}$ spin-chain system.

The lower panel of Fig. 2 is an expanded view of the susceptibility data below 60 K, showing the total $\chi(T)$ (filled circles), the χ_{chain} data (open circles), and a fit using the Johnston formula (solid line). It should be noted that even on this expanded scale, the overall agreement of the χ_{chain} data to the Johnston fitting is found to be good. However, below ~ 20 K a discrepancy between the experimental data and the fitted line appears. In fact, the change in the slope expected in the Johnston model around $T \sim 0.4J$ K (about 10 K in the present case) is not present in our data. Given the fact that $\text{Sr}_3\text{CuPtO}_6$ has an unconventional chain structure, some departures in the magnetic behavior from the theoretical model are not unexpected. Nevertheless, it must also be borne in mind that in the temperature range considered here, the χ_{chain} data are very sensitive to the subtraction of χ_{add} , which may introduce some uncertainty in the resulting χ_{chain} values.

In order to better understand the low-temperature behavior of $\text{Sr}_3\text{CuPtO}_6$, it is useful to investigate the temperature dependence of the heat capacity of this system, which is expected to be much less affected by additional contributions from broken chains or paramagnetic impurities.

B. Heat capacity

The total heat capacity of $\text{Sr}_3\text{CuPtO}_6$ as a function of temperature (1.9–300 K) is shown in Fig. 3(a) (inset). This data contain no signature of long-range magnetic ordering in this temperature range. Figure 3 also depicts the $C(T)$ of the nonmagnetic isostructural compounds $\text{Sr}_3\text{ZnPtO}_6$. At low temperatures (below about 50 K), $C_{tot}(\text{Sr}_3\text{CuPtO}_6)$ is larger in value than $C_{tot}(\text{Sr}_3\text{ZnPtO}_6)$. This is clearly due to an additional contribution to the heat capacity of magnetic origin for the Cu compound. It is expected that the magnetic contribution to $C_{tot}(\text{Sr}_3\text{CuPtO}_6)$ should tend to zero at high temperatures. There is a difference between $C_{tot}(\text{Sr}_3\text{ZnPtO}_6)$ and $C_{tot}(\text{Sr}_3\text{CuPtO}_6)$ even at 300 K, which is due to the mass difference of the Cu and the Zn atoms. In order to calculate the lattice contribution, C_{lat} , of $\text{Sr}_3\text{CuPtO}_6$ from the heat capacity data of $\text{Sr}_3\text{ZnPtO}_6$, a careful mass correction to the data is required. In the present case we have used a phenomenological scaling of the Debye temperature Θ_D with two scaling factors (see the Appendix) to obtain the C_{lat} from the heat capacity of the nonmagnetic reference sample. It should be noted that the scaling for C_{lat} has only a weak effect at low temperatures. $C_{lat}(\text{Sr}_3\text{CuPtO}_6)$ is almost superimposed onto $C_{tot}(\text{Sr}_3\text{ZnPtO}_6)$ below about 40 K. Since this is the region of interest for the analysis of the 1D magnetic features, these should not be significantly affected by any imperfection in the model used to derive $C_{lat}(\text{Sr}_3\text{CuPtO}_6)$.

The lower panel of Fig. 3 shows the magnetic contribution to the heat capacity of $\text{Sr}_3\text{CuPtO}_6$, $C_{mag}(T)$, that was obtained by subtracting the lattice contribution $C_{lat}(T)$ from the total heat capacity $C_{tot}(T)$. The main feature is a broad peak at low temperature, as expected in a 1D magnetic system.¹⁰ In their theoretical investigation of $S = \frac{1}{2}$ Heisenberg antiferromagnetic chains, Johnston *et al.*¹¹ have pro-

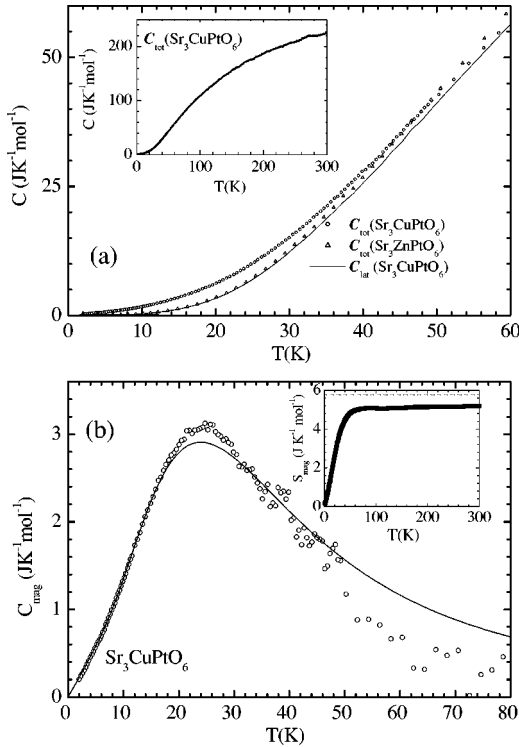


FIG. 3. The upper panel (a) shows the heat capacity vs temperature data of $\text{Sr}_3\text{CuPtO}_6$ in the temperature range 1.9–60 K. The heat capacity data of the nonmagnetic isostructural compound $\text{Sr}_3\text{ZnPtO}_6$ is also shown in the figure along with the lattice contribution of the heat capacity of $\text{Sr}_3\text{CuPtO}_6$ as calculated (see text for details) from the heat capacity data of $\text{Sr}_3\text{ZnPtO}_6$. The inset in the upper panel shows a full view (1.9–300 K) of the heat capacity vs temperature data of $\text{Sr}_3\text{CuPtO}_6$. The lower panel (b) shows the magnetic contribution to the heat capacity (C_{mag}) of $\text{Sr}_3\text{CuPtO}_6$ as a function of temperature along with the curve predicted by the Johnston model (solid line) for $J=25.5$ K. The inset shows the magnetic entropy vs temperature data for $\text{Sr}_3\text{CuPtO}_6$, and the dotted line in the inset denotes the theoretical value of the entropy ($R \ln 2$) for an $S=\frac{1}{2}$ system.

posed analytical expressions for the temperature dependence of the heat capacity. The solid line in Fig. 3 is the curve predicted by this model (Eqs. 54(a)–54(c) of Ref. 11) for $J=25.5$ K. It is worth emphasizing that there are no free parameters other than J in this model. On the scale of Fig. 3, only curves obtained using a narrow range (± 0.5 K) of J values around 25.5 K provide good overall agreement with the experimental data. The curve corresponding to $J=25.5$ K gives the best fit for $T < \frac{1}{2}J$ and the quality of the agreement is quite satisfactory up to about 40 K. Above $T \sim 50$ K, the $C_{\text{mag}}(T)$ data clearly depart from the model, a behavior which can be ascribed to the uncertainty in the estimation of C_{lat} (for instance, at $T \sim 60$ K, the expected magnetic contribution is just 2% of the measured total heat capacity). In the Bonner-Fisher model, the intrachain coupling is related to the temperature T_{max} corresponding to the maximum in $C_{\text{mag}}(T)$ data as $T_{\text{max}} \approx 0.962J$. Considering T_{max} in the range 24–25.5 K, one obtains a J value lying between 25 K and 26.5 K, which is in good agreement with the value of J given by the Johnston model above.

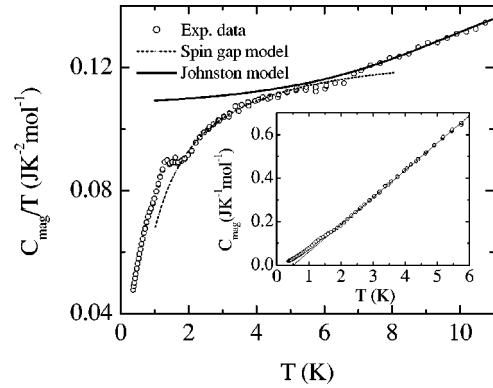


FIG. 4. The low-temperature (down to 0.35 K) magnetic heat capacity vs temperature data of $\text{Sr}_3\text{CuPtO}_6$ along with the curve (solid line) predicted by Johnston model (down to 1 K) for $J=25.5$ K and the curve (dotted line) obtained by fitting $C_{\text{mag}}^{\Delta} = \gamma_{\text{mag}}^{\Delta} T \exp(-\Delta/T)$ to our data in the temperature range 2–5 K and then extrapolated below and above 2 K and 5 K, respectively. The inset shows the C_{mag} vs T data below 6 K. The line emphasizes the quasilinear behavior of the data in the temperature range 2–6 K.

The inset in the lower panel of Fig. 3 displays the temperature dependence of the magnetic entropy derived by $S_{\text{mag}}(T) = \int_0^T [C_{\text{mag}}(T')/T'] dT'$.²⁰ One observes that the calculated entropy saturates slightly below the theoretical value, $R \ln 2 = 5.76$ J/mol K, expected for $S=1/2$. This apparent *missing* entropy probably just reflects the uncertainty in the estimation of $C_{\text{lat}}(T)$.

In order to get a more comprehensive view of the 1D magnetic behavior of $\text{Sr}_3\text{CuPtO}_6$, we have extended our heat capacity measurement down to 0.35 K. Figure 4 shows the C_{mag}/T versus T data below 11 K, while the inset in Fig. 4 shows the temperature dependence of the C_{mag} data below 6 K. Around 1.5 K, C_{mag} contains a small feature (which is more clearly visible in the C_{mag}/T versus T plot), and then tends smoothly to zero as T is decreased further. This may be a signature of three-dimensional long-range magnetic ordering or of a spin-Peierls-like transition. However, the occurrence of such a transition appears to be in contrast with the work of Irons *et al.*,⁷ who reported the absence of any anomaly in the ac susceptibility measurements down to 0.27 K on a polycrystalline sample of $\text{Sr}_3\text{CuPtO}_6$. In order to understand the significance of this feature, further investigations based on neutron-scattering measurements are required. For the present analysis, we decided to restrict ourselves to the temperature range $T \geq 2$ K, for which C_{mag} is presumably related to the short-range intrachain coupling only.

In case of an AFM spin-chain system such as $\text{Sr}_3\text{CuPtO}_6$, C_{mag} is expected to show a linear T dependence, $C_{\text{mag}} = \gamma_{\text{mag}} T$, at low temperatures (approximately, $T < J/5$ which is below 5 K in our case). Our $C_{\text{mag}}(T)$ data in Fig. 4 (inset) show a quasilinear behavior in the temperature range 2–6 K, but clearly extrapolates to a finite T intercept of about 0.5 K at $C_{\text{mag}}=0$. Such a behavior suggests the possibility of a small gap of $\Delta \sim 0.5$ K in the spin excitation spectrum. Although, a spin gap should not exist in the case of a uniform $S=\frac{1}{2}$ spin-chain system, the possibility of a gap cannot be ruled out in the case of $\text{Sr}_3\text{CuPtO}_6$, with its unconventional spin-chain structure.

In Fig. 4, we have shown C_{mag}/T behavior predicted by the Johnston model (down to $T=1$ K) with $J=25.5$ K along with the experimental data. While the Johnston model well represents the experimental data down to 5 K, a deviation is visible in the low-temperature data. The experimental C_{mag}/T contains a clear downward curvature below 5 K, which is absent in the Johnston model that shows a rather constant $C_{mag}(T)/T$ behavior consistent with the expected linear T dependence of the C_{mag} data in this temperature range (1–5 K). This departure from the Johnston model behavior around 5 K cannot be simply attributed to the small feature observed around 1.5 K. If a spin gap is responsible for such a departure, to a first approximation, it can be accounted by a phenomenological relation $C_{mag}^{\Delta}/T = \gamma_{mag}^{\Delta} \exp(-\Delta/T)$ at low temperatures. The dotted line in Fig. 4 shows the fitting of C_{mag}^{Δ}/T to the data in the temperature range 2–5 K along with an extrapolation slightly below and above 2 K and 5 K, respectively. The parameters estimated by the fitting are found to be $\gamma_{mag}^{\Delta} = 0.128 \text{ J K}^{-2} \text{ mol}^{-1}$ and $\Delta = 0.64$ K. This phenomenological spin gap model can account for the downward curvature in the $C_{mag}(T)/T$ data below 5 K. According to the Johnston model, for an $S = \frac{1}{2}$ AFM spin-chain, the coefficient of the linear term (γ_{mag}) in C_{mag} is related to the intrachain coupling parameter as $\gamma_{mag} = R/3J$, where R is the universal gas constant. Although, strictly speaking, this relation is valid for an ideal gapless spin-chain system, we have used the relation in the present context to estimate the value of J . The value of J , obtained by inserting the value of γ_{mag}^{Δ} in the above relation, is found to be 22.2 ± 0.5 K, which is close to the values of J obtained from other methods.

IV. DISCUSSION

The present magnetic susceptibility and heat capacity investigations on single crystals of $\text{Sr}_3\text{CuPtO}_6$ show that there is a good overall agreement between our experimental data and the theoretical predictions for an $S = \frac{1}{2}$ Heisenberg AFM spin-chain system. The values of the characteristic coupling parameter J , obtained from different measurements, are reasonably consistent.

Such a good agreement with standard spin-chain models is rather surprising for a compound whose one-dimensional magnetic character was recently questioned.^{3,7} The doubts raised were based upon the large value of the interchain coupling parameter J' , derived from an analysis of the magnetic susceptibility, leading to a ratio $J/J' \sim 3$. Our susceptibility analysis discussed so far in the text has been performed without considering any interchain coupling parameter (i.e., $J' = 0$). In order to get an idea of the interchain coupling parameter, we have reanalyzed our susceptibility data with the relation proposed by Hatfield⁶ and previously used by Claridge *et al.*³ We found that this mean-field approach can improve the quality of the fitting with the addition of an AFM interchain coupling parameter. The best fit is obtained for $J = 25.1 (\pm 0.1)$ K and $J' = 4.3 (\pm 0.2)$ K. The J' value is slightly less but still comparable with the value 7.3 K reported by Claridge *et al.*³ However, one should be careful in

interpreting the value of J' from this kind of analysis. For low-dimensional magnetic systems (with small and weakly T -dependent χ), the introduction of an additional fitting parameter J' can often lead to unphysical results. In the case of $\text{Sr}_3\text{CuPtO}_6$, such a large value of J' appears to be inconsistent with the global magnetic behavior, particularly the absence of long-range magnetic order down to 2 K. A finite value of the interchain coupling should eventually lead to a three-dimensional ordering at a temperature T_N and theoretical models have established relationships between T_N and the coupling parameters (J and J') for the weakly coupled linear-chain systems. For $S = \frac{1}{2}$ AFM Heisenberg chains, the model proposed by Oguchi,²¹ based on a Green's function method, has been used extensively.²² Recently, Schulz²³ has proposed another model relating T_N , J and J' for weakly coupled $S = \frac{1}{2}$ chains, which is based on a mean-field approximation for the interchain coupling and exact results for the resulting effective 1D problem. Both these models deal with a square lattice of the spin-chains and as outlined by Lines *et al.*,²⁴ corrections are required to apply these models to systems with a hexagonal arrangement of spin chains, as is the case for $\text{Sr}_3\text{CuPtO}_6$. With $J = 25.5$ K, and $T_N \leq 2$ K (since, there is no 3D order at least down to 2 K), both the Oguchi and the Schulz models predict an upper limit for the interchain coupling constant J' of 0.2 K. Therefore, it is clear that the large value of J' derived previously, by fitting the Hatfield model to the susceptibility data, may not be reliable. With $J' \leq 0.2$ K, one obtains the *lower boundary* of the ratio of the intrachain and interchain coupling parameters to be $\approx 130 (J/J' \geq 130)$ and this ratio is more consistent with the 1D magnetic character of $\text{Sr}_3\text{CuPtO}_6$.

Now the question is how to reconcile such a large J/J' ratio with the fact that the distance between two neighboring Cu^{2+} ions is approximately the same along and perpendicular to the chain. It is well known that the strength of the exchange coupling not only depends upon the distance but also on the nature of the exchange pathway. From the viewpoint of the mediation of the exchange interaction between Cu^{2+} ions, the situation is very different, parallel and perpendicular to the chains. Although the Pt^{4+} ions located in between the Cu^{2+} ions along the chains are in the low spin state ($S=0$), they possess unfilled $3d$ orbitals and can thus participate in the exchange interaction. A similar mechanism cannot be expected for the Sr^{2+} ions located in between the CuO_6 - PtO_6 chains. Such a difference in the exchange pathway can qualitatively explain the large J/J' ratio in $\text{Sr}_3\text{CuPtO}_6$.

Finally, let us consider the low-temperature (0.35–6 K) heat capacity data for $\text{Sr}_3\text{CuPtO}_6$, which revealed some deviation from the $S = \frac{1}{2}$ 1D AFM Heisenberg model. Although, they are also visible in χ_{chain} data (Fig. 3), such deviations can be studied more precisely in C_{mag} data. The latter data led us to propose the existence of a small energy gap in the spin excitation spectra. A uniform half-odd integral spin-chain system is supposed to be gapless.²⁵ One simple explanation for the origin of a small gap is a weak modulation in the strength of the exchange interaction along the chain.²⁶ The zigzag nature of the spin chain in $\text{Sr}_3\text{CuPtO}_6$

may result in such a modulation.²⁷

In conclusion, we have performed a detailed investigation of the magnetic susceptibility and the heat capacity behavior of the compound Sr₃CuPtO₆. The use of a nonmagnetic isostructural compound (Sr₃ZnPtO₆) has enabled us to extract the magnetic contribution to the heat capacity. Both the magnetic susceptibility and the heat capacity were found to be consistent with the Johnston and Bonner-Fisher models for an $S = \frac{1}{2}$ AFM spin chain, with similar values of the intrachain coupling parameters ($J \sim 25.5$ K). Based on the fact that there is no long-range magnetic order observed in this system, at least down to 2 K, the *lower limit* of the ratio of the intrachain and interchain coupling parameters is expected to be ~ 130 . These observations, in contrast to the previous reports,^{3,7} clearly identify Sr₃CuPtO₆ as an $S = \frac{1}{2}$ spin-chain compound with 1D magnetic character. Deviations from the 1D uniform $S = \frac{1}{2}$ Heisenberg models were observed in the low-temperature regime, which indicate the possible existence of a gap in the spin excitation spectrum.

ACKNOWLEDGMENT

We acknowledge the financial support of the EPSRC (UK) for this project.

APPENDIX: CALCULATION OF C_{lat}

According to the Debye model of lattice heat capacity,

$$C_{lat}(T) = 3pRD[\theta_D(T)/T], \quad (\text{A1})$$

where p is the number of atoms per molecule, R is the gas constant, $\theta_D(T)$ is the Debye temperature, and $D(x) = (3/x^3) \int_0^x [z^4 e^z / (1 - e^z)^2] dz$ is the Debye function. The problem of finding C_{lat} for a magnetic sample reduces to the problem of deriving the Debye temperature of the magnetic sample, $\theta_D^{sam}(T)$, from that of a nonmagnetic isostructural

reference compound, $\theta_D^{ref}(T)$, which can be directly derived from the total heat capacity $C_{tot}(T)$ of the reference sample by inverting Eq. (A1). A one-parameter scaling of the Debye temperature [$\theta_D^{sam}(T) = r\theta_D^{ref}(T)$] (where r is a constant) is found to be inadequate as there is no r value leading to $C_{lat}(\text{Sr}_3\text{CuPtO}_6)$ which tends to $C_{tot}(\text{Sr}_3\text{CuPtO}_6)$ at 300 K, while lying below it for $T < 300$ K. The former requirement is based on the fact that at 300 K, the theoretical magnetic contribution to the heat capacity for $S = \frac{1}{2}$ Heisenberg chain with $J \sim 25$ K is expected to be only 0.02% of the total heat capacity of Sr₃CuPtO₆. The failure of this one-parameter scaling led us to use an extension of this approach with two phenomenological factors, corresponding to the highest (T_H) and lowest (T_L) temperatures of our data. We can express $\theta_D^{ref}(T) = \theta_D^{ref}(T_L) + [\theta_D^{ref}(T_H) - \theta_D^{ref}(T_L)]f(T)$, where $f(T)$ is a function such as $f(T_L) = 0$ and $f(T_H) = 1$. Owing to the structural equivalence of the magnetic and the nonmagnetic reference compounds, we assumed that $\theta_D^{sam}(T)$ can be approximated by a similar expression, keeping the same function $f(T)$. The θ_D^{sam} values at T_L and T_H are related to their counterparts in the reference sample by two adjustable parameters: $\theta_D^{sam}(T_L) = r_1 \theta_D^{ref}(T_L)$ and $\theta_D^{sam}(T_H) = r_2 \theta_D^{ref}(T_H)$. The parameter r_2 was determined from the requirement that C_{mag} should vanish at T_H , resulting in a C_{lat} that tends to C_{tot} at T_H . For the present case of Sr₃CuPtO₆ with Sr₃ZnPtO₆ as the reference sample, the single parameter correction factor (r) (which is valid in the low- T region, i.e., $T \ll \Theta_D$ only) estimated from the difference in the mass of the atoms is almost equal to 1.²⁸ Therefore, the parameter r_1 was chosen as the smallest value for which C_{lat} does not cross C_{tot} over the whole T range. The estimated values of the parameters are $r_1 = 1.025$ and $r_2 = 1.050$ (with $T_L = 2$ K and $T_H = 300$ K). Figure 3 shows the corresponding lattice contribution of Sr₃CuPtO₆ that was obtained by including $\theta_D^{sam}(T)$ in the Debye formula.

*Permanent address: Laboratoire CRISMAT, UMR 6508, Boulevard du Maréchal Juin, 14050 Caen cedex, France.

¹K.E. Stitzer and H.-C. zur Loye, *Curr. Opin. Solid State Mater. Sci.* **5**, 535 (2001).

²T.N. Nguyen, D.M. Giaquinta, and H.-C. zur Loye, *Chem. Mater.* **6**, 1642 (1994).

³J. Claridge, R.C. Layland, W.H. Henley, and H.-C. zur Loye, *Chem. Mater.* **11**, 1376 (1999).

⁴T.N. Nguyen, P.A. Lee, and H.-C. zur Loye, *Science* **271**, 489 (1996).

⁵J.L. Hodeau, H.Y. Tu, P. Bordet, T. Fournier, P. Strobel, and M. Marezio, *Acta Crystallogr., Sect. B: Struct. Sci.* **48**, 1 (1992).

⁶W.E. Hatfield, *J. Appl. Phys.* **52**, 1985 (1981).

⁷S.H. Irons, T.D. Sangrey, K.M. Beauchamp, M.D. Smith, and H.C. zur Loye, *Phys. Rev. B* **61**, 11 594 (2000).

⁸A. Niazi, E.V. Sampathkumaran, P.L. Paulose, D. Eckert, A. Handstein, and K.-H. Müller, *Phys. Rev. B* **65**, 064418 (2002).

⁹V. Hardy, S. Lambert, M.R. Lees, and D.McK. Paul, *Phys. Rev. B* **68**, 014424 (2003).

¹⁰J.C. Bonner and M.E. Fisher, *Phys. Rev.* **135**, A640 (1964).

¹¹D.C. Johnston, R.K. Kremer, M. Troyer, X. Wang, A. Klümper,

S.L. Bud'ko, A.F. Panchula, and P.C. Canfield, *Phys. Rev. B* **61**, 9558 (2000).

¹²A. Klümper and D.C. Johnston, *Phys. Rev. Lett.* **84**, 4701 (2000).

¹³S. Eggert, I. Affleck, and M. Takahashi, *Phys. Rev. Lett.* **73**, 332 (1994).

¹⁴S. Lukyanov, *Nucl. Phys. B* **522**, 533 (1998).

¹⁵C. Lampe-Önnerud, M. Sigrist, and H.-C. zur Loye, *J. Solid State Chem.* **127**, 25 (1996).

¹⁶M. Matsuda and K. Katsumata, *Phys. Rev. B* **53**, 12 201 (1996).

¹⁷V. Kiryukhin, Y.J. Kim, K.J. Thomas, F.C. Chou, R.W. Erwin, Q. Huang, M.A. Kastner, and R.J. Birgeneau, *Phys. Rev. B* **63**, 144418 (2001).

¹⁸Y. Liu, J.E. Drumheller, and R.D. Willett, *Phys. Rev. B* **52**, 15 327 (1995).

¹⁹N. Motoyama, H. Eisaki, and S. Uchida, *Phys. Rev. Lett.* **76**, 3212 (1996).

²⁰In order to calculate S_{mag} , we have used our $C_{mag}(T)$ data in the temperature range 0.35–300 K and extrapolated down to 0 K.

²¹T. Oguchi, *Phys. Rev.* **133**, A1098 (1964).

²²L.J. De Jongh and A.R. Miedema, *Adv. Phys.* **23**, 1 (1974).

²³H.J. Schulz, *Phys. Rev. Lett.* **77**, 2790 (1996).

²⁴M.E. Lines and M. Eibschütz, Phys. Rev. B **11**, 4583 (1975).

²⁵E. Lieb, T.D. Schulz, and D.C. Mattis, Ann. Phys. (N.Y.) **16**, 407 (1961).

²⁶J.C. Bonner and H.W.J. Blöte, Phys. Rev. B **25**, 6959 (1982).

²⁷R. L. Carlin, *Magnetochemistry* (Springer-Verlag, Berlin, 1986), p. 75.

²⁸M. Bouvier, P. Lethuillier, and D. Schmitt, Phys. Rev. B **43**, 13 137 (1991).